Max-Planck-Institut für Meteorologie

REPORT No. 329

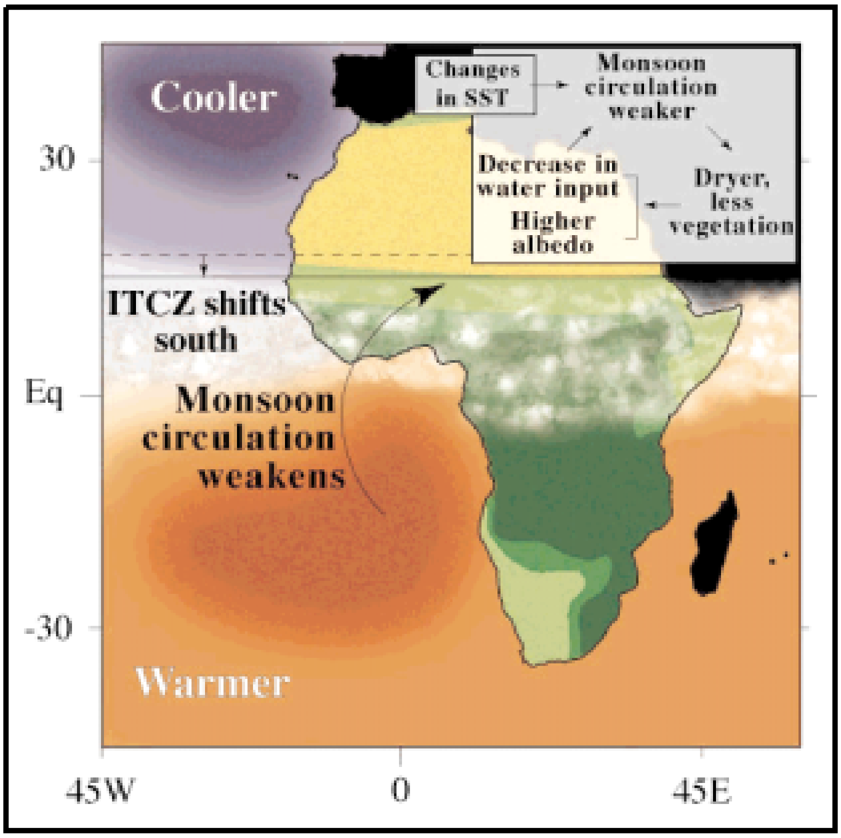

VEGETATION FEEDBACK ON SAHELIAN RAINFALL VARIABILITY IN A COUPLED CLIMATE LAND - VEGETATION MODEL

by

Karl-Georg Schnitzler • Wolfgang Knorr • Mojib Latif • Jürgen Bader • Ning Zeng

HAMBURG, September 2001

AUTHORS:

Mojib Latif
Jürgen Bader

Max-Planck-Institut
für Meteorologie

Karl-Georg Schnitzler
Wolfgang Knorr

Max-Planck-Institute
for Biogeochemistry
Jena
Germany

Ning Zeng

Dept.of Meteorology and
Earth System Science Interdisc. Center
University of Maryland
USA

MAX-PLANCK-INSTITUT
FÜR METEOROLOGIE
BUNDESSTRASSE 55
D - 20146 HAMBURG
GERMANY

Tel.: +49-(0)40-4 11 73-0
Telefax: +49-(0)40-4 11 73-298
E-Mail: <name> @ dkrz.de

REPb 329

Vegetation Feedback on Sahelian Rainfall Variability in a Coupled Climate Land-Vegetation Model

Karl-Georg Schnitzler, Wolfgang Knorr

Max-Planck-Institute for Biogeochemistry, Jena, Germany

Mojib Latif, Jürgen Bader

Max-Planck-Institute for Meteorology, Hamburg, Germany

Ning Zeng

Dept. of Meteorology and Earth System Science Interdisc. Center, University of Maryland, USA

submitted to Geophysical Research Letters (August, 2001)

ISSN 0937 - 1060

1 Abstract

Rainfall variability in the Sahel region shows a dramatic drying trend from the 1950s to the 1980s. Yet, most atmospheric general circulation models (AGCM) forced by observed sea surface temperatures (SSTs) were not able to reproduce the amplitude of this multi-decadal variation. Here, we investigate the sensitivity of Sahelian rainfall to vegetation-atmosphere interaction. We coupled the simple dynamic vegetation model (SVege) and the ECHAM4-AGCM and forced the system by observed SSTs. We show that vegetation-climate feedbacks amplify the decadal rainfall variability and that the coupled system simulates realistically the observed multi-decadal variations in Sahelian precipitation.

2 Introduction

The Sahelian region is one of the most climatically sensitive and ecologically unstable regions. It exhibits strong variability in both precipitation and vegetation on interannual and interdecadal timescales [*e.g. Nicholson et al.,* 1998]. FIG. 1d shows the observed rainfall anomalies over the Sahel from 1951 to 1994 [*Hulme,* 1998], with a pronounced drying trend starting in the 1950s and ending in the mid 1980s.

The reason for this trend is still a matter of intensive scientific debate [*e.g. Rowell et al.,* 1995, *Rowell,* 1996, *Ward,* 1998]. Possible explanations are: a modification of the surface albedo and surface evapotranspiration through desertification processes [*Charney,* 1975, *Xue & Shukla,* 1993, *Zheng & Eltahir,* 1997, *Xue,* 1997, *Zheng & Elthaier,* 1998] and SST anomalies [*Folland et al.,* 1986, *Xue & Shukla,* 1998].

Some AGCM simulations driven with observed SST have failed to simulate the magnitude of the Sahelian precipitation anomaly of the last 50 years [*Zeng et al.,* 1999], [ECHAM: FIG. 1a]. Recently, the studies of *Zeng et al.* [1999] and *Wang & Eltahir* [2000] have demonstrated that the coupled atmosphere-vegetation system tends to enhance climate variability arising from other slow components of the climate system such as the oceans. SST anomalies, for instance, can lead to a weaker monsoon, which causes less precipitation in the north African region. A dryer climate leads to less vegetation, which results in a higher albedo and reduced evapotranspiration by plants. Less water input into the atmosphere and a higher albedo will further weaken the monsoon.

3 Models and Experiments

To further test and explore this hypothesis we coupled the Hamburg AGCM ECHAM4 [*Roeckner et al.,* 1996] with the simple dynamic vegetation model SVege [*Zeng et al.,* 1999, *Zeng & Neelin,* 2000]. The coupled system was forced by observed SSTs (GISST 2.3) from 1945 to 1998 [*Rayner et al.,* 1996].

3.1 The general circulation model

The ECHAM4 physics and model performance are described in [*Roeckner et al.,* 1996]. Here, we use the model at T42 resolution (approx. 2.8 by 2.8 deg). The standard ECHAM4 model uses a fixed annual mean vegetation cover and static leaf area index (LAI). Evapotranspiration consists of the four fractions: Evaporation from bare soil, interception evaporation, snow sublimation, and leaf transpiration. The latter depends on energy balance, plant available soil water content, and fractional vegetation cover C_v, and is computed with a bucket scheme. Water holding capacity is prescribed as a function of soil texture and root depth. In the standard version, the prescribed surface albedo is interactively modified by simulated snow and ice cover, only.

3.2 The simple dynamic vegetation model

On annual to decadal timescales, vegetation growth in the tropics and subtropics responds mainly to the annual cycle of water availability and to a lesser extent to changes in radiation, temperature, and nutrients. In the simple dynamic vegetation model SVege, leaf area index and fractional cover vary with normalized vegetation growth and vegetation loss (dV/dt), modified by the relative amount of plant available soil water, w:

$$\frac{dV}{dt} = \frac{\omega}{\tau} * (1 - e^{-k*LAI}) - \frac{V}{\tau} \tag{1}$$

Here $k = 0.5$ denotes the extinction coefficient, LAI the leaf area index and $\tau = 1$ month the vegetation response timescale. V ranges between $]0, 1[$ and the LAI is assumed to be directly proportional to V:

$$LAI = LAI_{max} * V \tag{2}$$

with $LAI_{max} = 8.4 m^2/m^2$. Fractional vegetation cover is computed from an empirical relation [*Monteith,* 1973] to ensure consistency with LAI:

$$C_v = 1 - e^{-0.3*LAI} \tag{3}$$

Besides modifying the evapotranspiration through (2) and (3), the dynamic land vegetation changes the surface albedo, A, through

$$A = 0.48 - 0.4 * (1 - e^{-k*LAI}) \tag{4}$$

This yields a minimum albedo of 0.08 at $V = 1$ (dense forest) and a maximum albedo of 0.48 at $V = 0$ (full desert) [*Pinty et al.*, 2000]. This maximum value is somewhat higher than the original version used in [*Zeng et al.*, 1999].

3.3 The coupled system

In the coupled model, vegetation cover and leaf area index are calculated by the dynamic vegetation model in the region 45N-45S. Outside this domain, the original land model is used with fixed vegetation. The two main effects of vegetation dynamics that feed back onto the physical climate system are retained here: evapotranspiration and modification of surface albedo. Secondary effects like variation of surface roughness or modification of hydrological soil properties are not considered in this study. Three different ensemble integrations are forced by observed SST:
(a) ECHAM4 standard version: 4 realizations.
(b) ECHAM4 with static mean vegetation: The mean annual LAI and C_v, were derived from the ensemble mean output of the coupled runs under (c): 2 realizations.
(c) ECHAM4 coupled to SVege: 4 realizations.

4 Results

We focus our analysis on the Sahel region, here defined as the area extending from the African west coast to 20E and 13N to 20N.

The Sahel rainfall for the period 1950 to 1994 from the standard ECHAM4 ensemble amounts to 534 mm/year, an overestimation compared to the observational estimate of 354 mm/year. The coupled atmosphere-vegetation model ensemble has a mean of 573 mm/year, indicating a 'climate drift' of the coupled model. The fixed mean vegetation ensemble is even wetter with 626 mm/year.

Concerning the interdecadal variability, the realizations show good reproducibility, indicating a strong impact of the slowly changing SST boundary conditions on the precipitation anomalies (FIG. 1a-c).

The AGCM forced by observed SST alone is not able to reproduce the observed strength of the multi-decadal variability (FIG. 1a). This is also true for the run with changed (but fixed) vegetation (FIG. 1b). The coupled model (FIG. 1c), however, reproduces the multi-decadal variability in Sahelian rainfall very well. Our AGCM results are consistent with findings of *Zeng et al.* [1999] and *Wang & Eltahir* [2000].

The observed and simulated rainfall over northwest Africa averaged over the period 1951-1994 is shown in FIG.2, together with zonally averaged albedo (observed albedo of year 1996 is taken from [*Knorr et al.,* in press]). The ECHAM4 standard ensemble mean (FIG. 2a) shows an overestimation of the annual mean precipitation in both, the Sahel and in the Sahara regions compared to observations (FIG. 2d). The spatial rainfall pattern is improved considerably when we exchange ECHAM's default ('control') albedo by the mean albedo predicted by the vegetation model ('fixed'): This is because the increased albedo in the desert regions reduces rainfall and thus leads to a better savanna-desert gradient. While the savanna-desert transition (somewhat arbitrarily chosen at 400 mm in annual rainfall) is still located too far north, the sharp albedo increase northward across this boundary is simulated more realistically (only one year of albedo data were available, and we assume that interannual albedo changes are small compared to those large-scale features). The result is less precipitation in the desert [*Knorr et al.,* in press] and, across the boundary, a steeper and more consistent meridional precipitation gradient.

By definition, the albedo distribution of the coupled model including dynamic vegetation is the same as in the fixed vegetation case. Nevertheless, an interactively varying vegetation (FIG. 2c) leads to an even improved simulation of the mean precipitation, with a dryer Sahara compared to the fixed vegetation experiment.

We now discuss the underlying physical processes: It is obvious that the SST signal carries the information of the multi-decadal variability. The prescription of SST alone, however, does not reproduce the observed amplitude. Three components change going from fixed to dynamic vegetation runs:
1. the variable amplitude of the albedo annual cycle,
2. the interdecadal albedo trend, and
3. the variation of the transpiration area (LAI).

The combination of these processes enhances the SST induced signal. FIG.3

shows the annual cycle of the Sahelian albedo (upper plot). At the start of the monsoon season in June, the albedo of the dynamic vegetation run is always higher than in the fixed vegetation run. This implies a weakening of the monsoon, with less precipitation at the beginning of the monsoon season. This amplifies the SST-effect, which can be seen in the precipitation difference between the fixed and the dynamic run for the dry years (FIG. 3, lower plot).

On the other hand, during wet years, the monsoon strength at the end of the season is amplified by stronger evapotranspiration and convective precipitation related to higher LAI. This enhances precipitation especially at the end of the monsoon season (FIG.3, lower plot).

Since the vegetation timescale used in the model is 1 month, there is little information carried from one year to the next due to vegetation memory. Thus, the amplification of the interdecadal change in rainfall is due to a changing vegetation in near-equilibrium with precipitation. While in nature vegetation does have dynamic processes with longer timescales, the interdecadal variability does not require information to be carried from one to the next year as proposed e.g. by *Wang & Eltahir* [2000], since the low-frequency information is contained in the SST.

5 Conclusions

So far, most AGCM simulations were unable to reproduce the amplitude of the Sahelian drying trend from the 1950s to 1980s when forced by the observed SSTs. We have demonstrated that interactive coupling of the ECHAM4 AGCM with a dynamic vegetation model leads to considerable improvements in the spatial and temporal characteristics of rainfall simulation, with a wetter climate in the Sahel and a dryer Sahara compared to the standard model. More importantly, the same coupled model is able to correctly simulate the magnitude of the interdecadal rainfall changes in the Sahel. Vegetation responding dynamically to precipitation changes acts as an amplifier for a low-frequency (i.e. interdecadal) signal delivered by SST anomalies. The results support the notion that vegetation-atmosphere feedback plays an important role for understanding climate variability.

6 Acknowledgments

We are grateful to the EUMETSAT team and Yves Govaerts for data and discussion. N.Z.'s participation was supported by a fellowship from the Alexander von Humbolt foundation. This work was supported by the European Unions's PROMISE project and by the GLOWA project of the German Government.

Literatur

[*Charney,* 1975] Charney, J.G., Dynamics of deserts and droughts in Sahel, *Quart.J.Roy.Meteor.Soc., 101*, 193-202, 1975

[*Folland et al.,* 1986] Folland, C.K., T.N. Palmer, D.E. Parker, Sahel rainfall and worldwide sea temperatures, 1901-1985, *Nature, 320*, 602-607, 1986

[*Hulme,* 1998] Hulme, M., T.J.Osborn, T.C. Johns, Precipitation sensitivity to global warming: Comparison of observations with HadCM2 simulations, *Geophys.Res.Let.*, 3379-3382, 1998

[*Knorr et al.,* in press] Knorr, W., K.-G. Schnitzler and Y. Govaerts, The role of bright desert regions in shaping North African climate, *J.Res.Let.*, in press

[*Monteith,* 1973] Monteith, J.R., *Principals of environmental physics*, Elsevier, New York, 1973

[*e.g. Nicholson et al.,* 1998] Nicholson, S.E., C.J. Tucker, M.B. Ba, Desertification, drought, and surface vegetation: An example from the West African Sahel, *Bull.Amer.Meteor.Soc.*, 79, 815-829, 1998

[*Pinty et al.,* 2000] Pinty, B., F. Roveda, M.M. Verstraete, N. Gobron, Y. Govaerts, J.V. Martonchik, D.J. Diner and R.A. Kahn, Surface albedo retrieval from Meteosat - 2. Applications, *J.Geophys.Res.*, 105, 18113-18134, 2000

[*Rayner et al.,* 1996] Rayner, N.A., E.B. Horton, D.E. Parker, C.K. Folland, R.B. Hackett, Version 2.2 of the global sea-ice and sea surface temperature data set, 1903-1994, *Clim. Res. Tech. Note 74,* CRTN74, U.K. Meteorol. Office, Bracknell, Berkshire, England, 1996

[*Roeckner et al.,* 1996] Roeckner, E., K. Arpe, L. Bengtsson, M. Christoph, M. Claussen, L. DYmenil, M. Esch, M. Giorgetta, U. Schlese, U. Schulzweida, The atmospheric general circulation model ECHAM-4: Model description and simulation of present-day climate, *MPI Report No. 218*, Max-Planck-Institute for Meteorology, Hamburg, Germany, 1996

[*e.g. Rowell et al.,* 1995] Rowell, D.P., C.K. Folland, K. Maskell, M.N. Ward, Variability of summer rainfall over tropical north Africa (1902-92): Observations and modelling, *Quart.J.Roy.Soc.*, 121, Part A, 669-704, 1995

[*Rowell,* 1996] Rowell, D.P. (1996): Variability of summer rainfall over tropical north Africa (1902-92): Observations and modelling - further analysis of simulated interdecadal and interannual variability of summer rainfall over tropical North Africa, *Quart.J.Roy.Soc., 122*, 1007-1013, 1996

[*Wang & Eltahir,* 2000] Wang, G., E.A.B. Eltahir, Role of vegetation dynamics in enhancing the low frequency variability of the Sahelian rainfall, *Water Resources. Res.,36*,No.4, 1013-1021, 2000

[*Ward,* 1998] Ward, M.N., Diagnosis and short-lead time prediction of summer rainfall in tropical North Africa at interannual and multi-decadal timescales, *J. Climate, 11*, 3167-3191, 1998

[*Xue & Shukla,* 1993] Xue, Y., J. Shukla, The influence of land surface properties on Sahel climate. Part I: Desertification, *J. Climate, 5*, 2232-2245, 1993

[*Xue,* 1997] Xue, Y., Biosphere feedback on regional climate in tropical North Africa, *Q.J.R. Meteorol. Soc., 123*, 1483-1515, 1997

[*Xue & Shukla,* 1998] Xue, Y., J. Shukla, Model simulations of the influence of global SST anomalies on Sahel rainfall, *Mon.Wea.Rev., 126*, 2782-2792, 1998

[*Zeng et al.,* 1999] Zeng, N., J.D. Neelin, K.-M. Lau, C.J. Tucker, Enhancement of interdecadal climate variability in the Sahel by vegetation interaction, *Science 286*, 1537-1540, 1999

[*Zeng & Neelin,* 2000] Zeng, N., J.D. Neelin, The role of Vegetation-Climate Interaction and Interannual Variability in Shaping the African Savanna, *J. Climate, 13*, 2665-2670, 2000

[*Zheng & Eltahir,* 1997] Zheng X, E.A.B. Eltahir, The response to deforestation and desertification in a model of West African monsoons, *Geophys. Res. Lett., 24*, 155-158, 1997

[*Zheng & Elthaier,* 1998] Zheng, X., E.A.B. Eltahir, The role of vegetation in the dynamics of West African monsoons, *J. Clim., 11* , 2078-2096, 1998

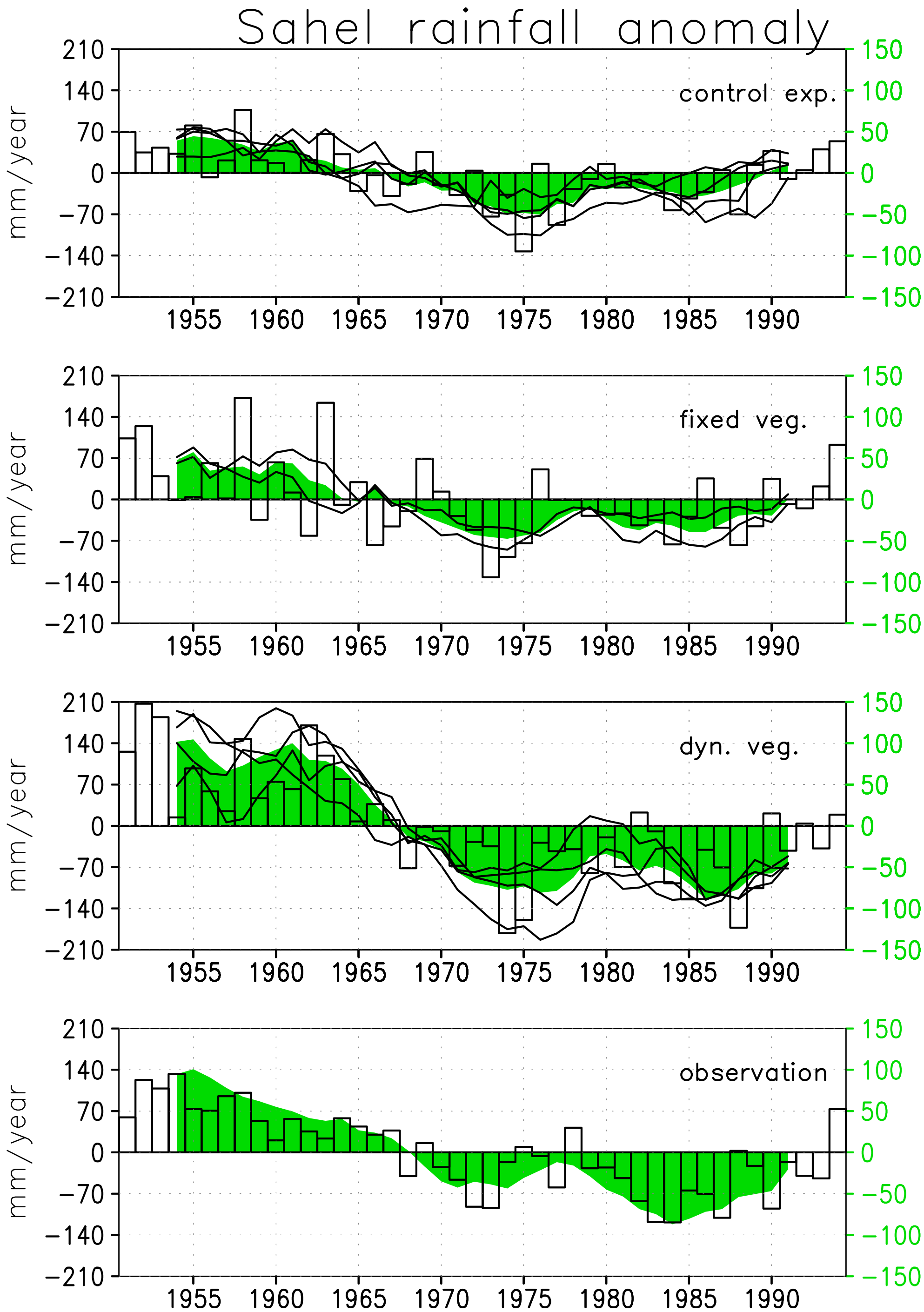

FIGURE 1: Sahel rainfall anomalies relative to the 1951-1994 mean. White bars: annual mean (left axis). Shaded curve: 7 year running mean of the ensemble (right axis). Lines: 7 year running mean, single realizations of the ensemble (right axis).

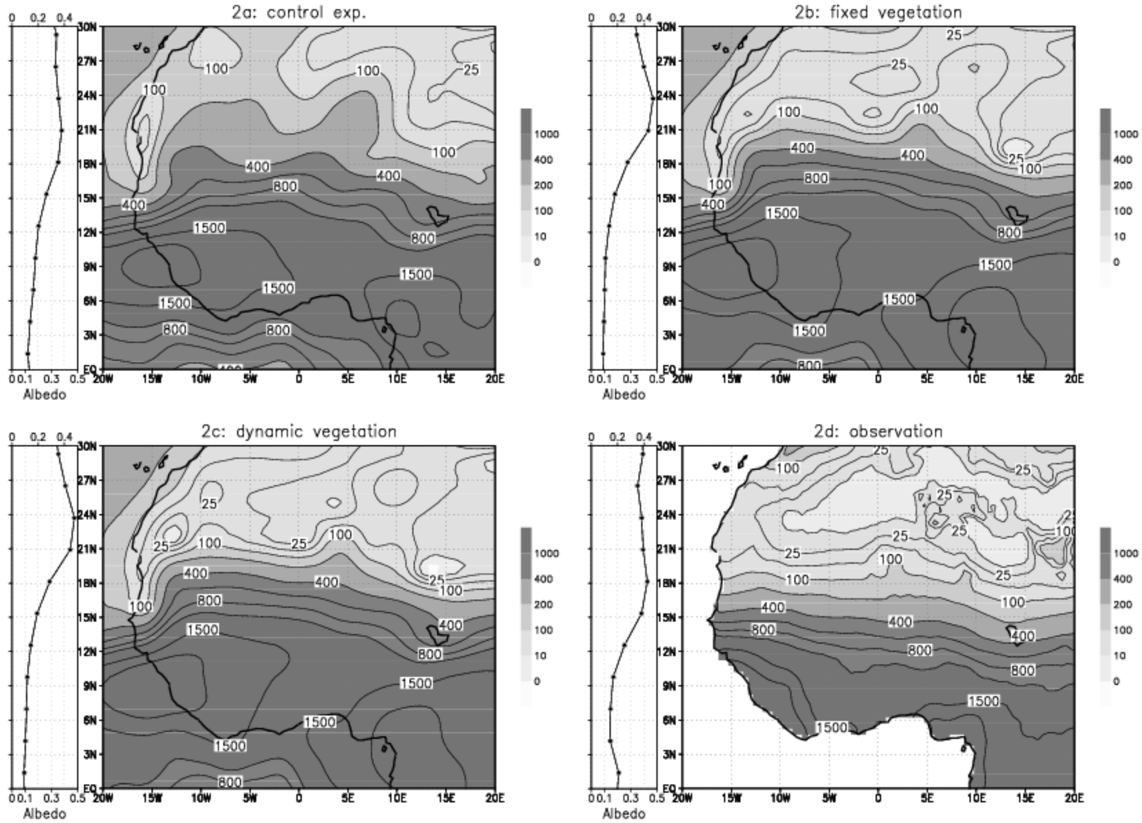

FIGURE 2: Mean rainfall distribution from 1951 to 1994 [mm/year]. On the left side of each plot, the zonal and temporal mean value of surface albedo is shown (all yeas for simulations, 1996 for satellite observations with Meteosat).

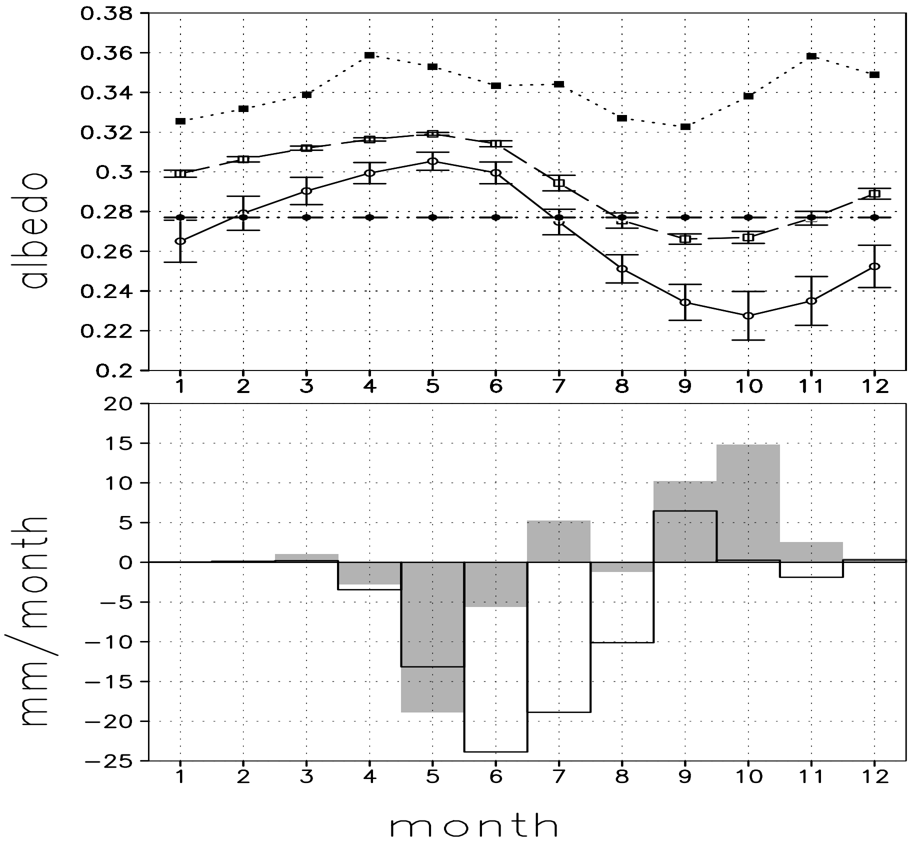

FIGURE 3: Upper panel: Annual cycle of surface albedo at 400mm/year precipitation latitude. Dotted: Meteosat (only 1996), solid line: wet years (1951-56), dashed line: dry years (1980-85). Staight line at 0.268: Mean static albedo from fixed vegetation runs. Lower panel: Anual cycle of precipitation difference between static vegetation and dynamic vegetation ensembles. (white: dry years, grey: wet years).